Influence of pattern corrosion on the time-dependent cyclic behavior of RC bridge columns

Angelo Pelle[1], Bruno Briseghella[2], Carlotta Contiguglia[1], Alessandro V. Bergami[1], Gabriele Fiorentino[3], Gian Felice Giaccu[4], Davide Lavorato[1], Giuseppe Quaranta[5], Alessandro Rasulo[6] and Camillo Nuti[1]

[1] Roma Tre University
Department of Architecture
Rome, Italy

[2] Fuzhou University
College of Civil Engineering
Fuzhou, China

[3] University of Bristol
Department of Civil Engineering
Bristol, UK

[4] University of Sassari
Department of Architecture, Design and Urban Planning,
Alghero, Italy

[5] Sapienza University of Rome
Department of Structural and Geotechnical Engineering
Rome, Italy

[6] University of Cassino and Southern Lazio,
Department of Civil and Mechanical Engineering
Cassino, Italy

Mail address: angelo.pelle@uniroma3.it

Abstract
This study is meant at understanding the influence of the pattern of corrosion due to chlorides-induced corrosion on the time-dependent cyclic behavior of reinforced concrete (RC) bridge columns. The chloride ingress in the cross-section of the column is simulated by a multiphysics FE approach taking into account both environmental and material factors. The non-linear cyclic responses of the RC bridge column under corrosion is evaluated by a nonlinear fiber model. A parametric study is finally conducted for a real case study, which aims at unfolding the role of the corrosion pattern on the time variation of capacity and ductility.

1 Introduction

Bridge structures are of crucial importance for the social and economic impact on the community, particularly for those located along key routes. RC bridges may be subjected to deterioration phenomena which significantly reduce their structural safety in a short time, among these the corrosion of steel reinforcement is the most important one.

Localized corrosion due to chloride ions may be very severe for RC elements and thus deserves some consideration. A recent study showed that the durability of the bridges is considerably affected by sea chloride [1]. This has motivated several studies in recent years on this topic.

On the one side, approaches based on multiphysics analysis have been proposed to evaluate the time-dependent evolution of the steel corrosion in RC elements [2]-[4]. On the other side, several studies have focused their attention on the numerical modelling of corroded RC bridge components [5]-[11].

The present work investigates the long-term behaviour of a real RC bridge column under chloride-induced corrosion. Firstly, a multiphysics simulation is adopted to evaluate the evolution of steel corrosion during the time. Next, the nonlinear modelling of the RC bridge column is addressed. Finally, the results obtained are discussed.

2 Chloride ingress and corrosion current density in RC bridge column

The ingress of chloride ions inside concrete cover is simulated by a multiphysics FE-based approach. Chloride penetration in concrete is approximated as a diffusion process. Fick's second law of diffusion can be adopted to simulate the diffusion of chloride ions into concrete cover in the time *t*, that is:

$$\frac{\partial C_{\mathrm{tc}}}{\partial t} = \frac{\partial}{\partial x}\left(D_c^* \frac{\partial C_{\mathrm{fc}}}{\partial x}\right) + \frac{\partial}{\partial y}\left(D_c^* \frac{\partial C_{\mathrm{fc}}}{\partial y}\right) \tag{1}$$

where C_{tc} is the total chloride concentration, C_{fc} is the concentration of chloride dissolved in the pore solution, D_c^* is the apparent chloride diffusion coefficient which can be evaluated with equation (2).

$$D_{\mathrm{c}}^* = \frac{D_c}{1 + \frac{1}{\omega_e}\frac{\partial C_{bc}}{\partial C_{fc}}} \tag{2}$$

where D_{c} is the effective chloride diffusion coefficient, ω_{e} is the water held in both capillary and gel pores and $\partial C_{bc}/\partial C_{fc}$ is known as blinding capacity.

The effective coefficient of diffusion is affected by several physical, chemical, and mechanical phenomena. In the present work the effect of temperature, pore relative humidity, cover crack width, and concrete age are taken into account.

The partial nonlinear equations are solved through by means of the program COMSOL Multiphysics 5.3 and the corrosion current density i_{corr} is correlated with chloride concentration by: [12]

$$\ln 1.08 i_{\mathrm{corr}} = 7.89 + 0.7771 \ln 1.69 C_{\mathrm{tc}} - \frac{3006}{T} - 0.000116 R_{\mathrm{c}} + 2.24 t^{-0.215} \tag{3}$$

where T is the temperature, R_{c} is the ohmic resistance of concrete, and t is in years. The complete formulation is reported in [11].

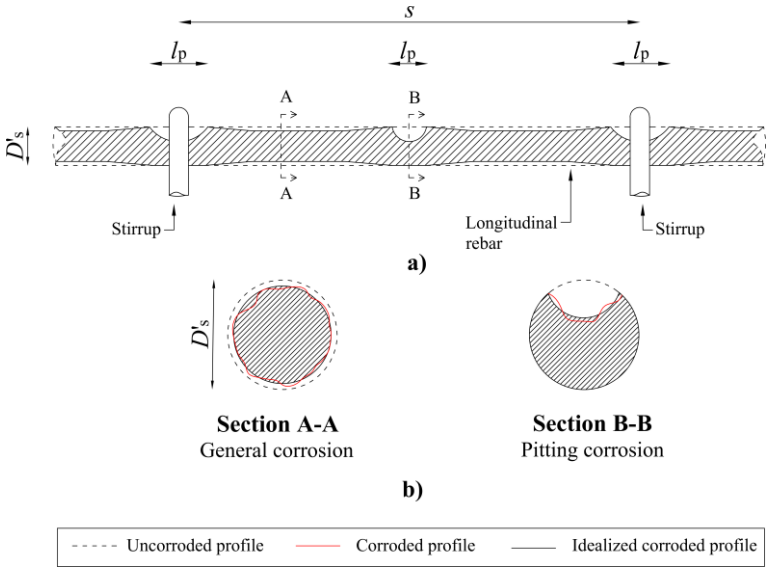

Fig. 1 Schematic view of the corrosion pattern.

3 Corrosion pattern and structural modelling of corroded RC bridge columns

This section illustrates as the effects of chloride-induced corrosion are evaluated, together with the nonlinear FE model developed to simulate the cyclic response of RC bridge column.

3.1 Corrosion Pattern

Localized corrosion, due to chloride ions, takes place together with generalized corrosion [13],[14], as shown in Fig. 1. Hence, corrosion pattern is expected to affect the structural response of RC members.

As regards, the increment of pit depth Δp [mm] for the localized corrosion is evaluated as follows:

$$\Delta p = 0.0116 i_{corr} \Delta t R \tag{4}$$

where Δt [years] is the time step, and R is the pitting factor (assumed to lie between 6 and 8). At each time instant, pit depth p [mm] is obtained as the cumulative sum of previous increments Δp. Then, the area of the corroded reinforcing steel bar A_t^p is evaluated by means of the hemispherical model proposed by Val and Melchers [15].

The generalized corrosion is idealized as a uniform reduction of the rebar cross-section area. In the present work, the loss cross-section area of the rebar under generalized corrosion A_g is parameterized as follows:

$$A_g = \rho A_p \tag{5}$$

where A_p is the loss cross-section area of the rebar under localized corrosion. If $\rho = 1$ the magnitude of generalized and localized corrosion is the same. Conversely, if $\rho = 0$ the generalized corrosion is negligible.

3.2 Stress-strain relationship for bare steel bare

Models of bare steel bar in tension and compression are here introduced, they serve to identify the main parameters of constitutive law involved in the nonlinear modelling of RC bridge columns.

The failure condition of the corroded rebar under tension corresponds to the attainment of the ultimate strain ε'_{su} in the pit, thus the average strain ε_{su} over the reference length L (i.e. L is assumed to be equal to the stirrup spacing s) can be evaluated as follows:

$$\varepsilon_{su} = \frac{\varepsilon'_{su} l_p + \varepsilon_s^g (L - l_p)}{L} \tag{6}$$

where l_p is the pit length, ε'_{su} is the ultimate strain of the uncorroded steel, and ε_s^g is the strain level in the reinforcing steel bar under generalized corrosion, which can be evaluated as described in [11].

Regarding the behaviour of the bare steel bar under compression, a numerical model developed into OpenSEES is adopted to calibrate the parameter of the constitutive law. The adopted buckling length L_b to evaluate the bare steel bar response under compression is equal to the distance between transverse reinforcement s (local buckling) or to an integer multiple of it (global buckling). The global buckling takes place when the loss of the cross-section area of transverse reinforcement due to corrosion is high, and confinement of longitudinal bar cannot be anymore sustained by it. Hence, the buckling length of longitudinal reinforcement may increase over time.

3.3 Numerical FE model of RC bridge column

The nonlinear FE model of the RC bridge column has been developed into OpenSEES platform. Kashani et al. [5] recommended assuming the integration length of the first integration point equal to L_b to overcome the lack of objectivity at local or global level for force-based elements [16]. For this reason, the model adopts two force-based fiber elements (Fig. 2) where the lower element has, in case of local buckling, a length equal to $6L_b$ and three Gauss-Lobatto integration points. Conversely, in case of global buckling, it has a length equal to $2L_b$ and two Newton-Cotes integration points.

Moreover, a rigid link is introduced to connect the column tip with the point where axial and lateral forces are applied. A zero-length section at the base of the column is used to simulate the strain-penetration of the anchorage reinforcement in the footing. In the zero-length section, the slip-stress proposed by Zhao and Sritharan [17] is employed for the reinforcing steel bars assumed to be uncorroded in the

footing. Instead, the recommendations proposed by Kashani et al. and Berry et al. [5],[18] are adopted for the concrete.

The uniaxial material Concrete01 available in the OpenSEES material library is adopted to simulate the response of the unconfined cover concrete. The effect of cover cracking and spalling on the cover concrete due to rust expansion are also taken into account as suggested by Coronelli and Gambarova [19]. Instead, the uniaxial material Concrete04 is employed to simulate the response of the confined core concrete. The effect of the transverse reinforcement corrosion on core confinement is modelled by referring to the corroded cross-section area of the transversal reinforcement.

The constitutive law adopted for the longitudinal reinforcement is the modified Monti-Nuti steel model, its complete formulation is available in [20]-[22]. The model has been developed ad hoc into OpenSEES, but it is not publicly available in the library material of the OpenSEES yet.

Furthermore, the iterative procedure proposed by Dhakal and Maekawa [23] and later implemented by Kashani et al. [24] for corroded rebars is employed to evaluate the effective buckling length.

4 Numerical investigation

4.1 Case study

The selected bridge column modelled in the present study is shown in Fig. 3. It is derived from a real RC bridge located in Sardinia (Italy). The column has a height of 3.85 m and a circular cross-section with a diameter equal to 1.2 m. The reinforcement layout consists of 20 steel rebars with an uncorroded diameter D'_s equal to 24 mm arranged on a single concentric circular layer. Moreover, there is a spiral confinement whose diameter and spacing are equal to 12 mm and 250 mm, respectively. The concrete cover is equal to 40 mm, and the axial load on the single column P is estimated to be equal to 4500 kN.

Mechanical proprieties of concrete are assumed to be f'_c = 30 MPa and ε'_c = 0.2%. Average uncorroded mechanical proprieties of the reinforcing steel bar are assumed to be f'_{sy} = 536 MPa, f'_{su} = 649 MPa and ε'_{su} = 11.6%.

The pier is modelled in the longitudinal direction, hence, it can be effectively modelled as a cantilever element.

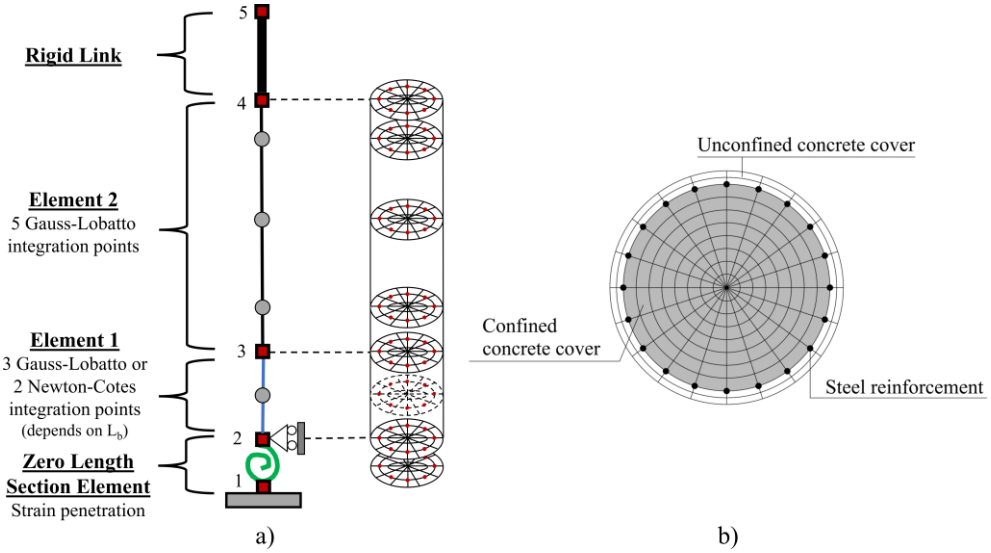

Fig. 2 a) Structural FE model of the RC bridge column; b) Detail of the cross-section discretization

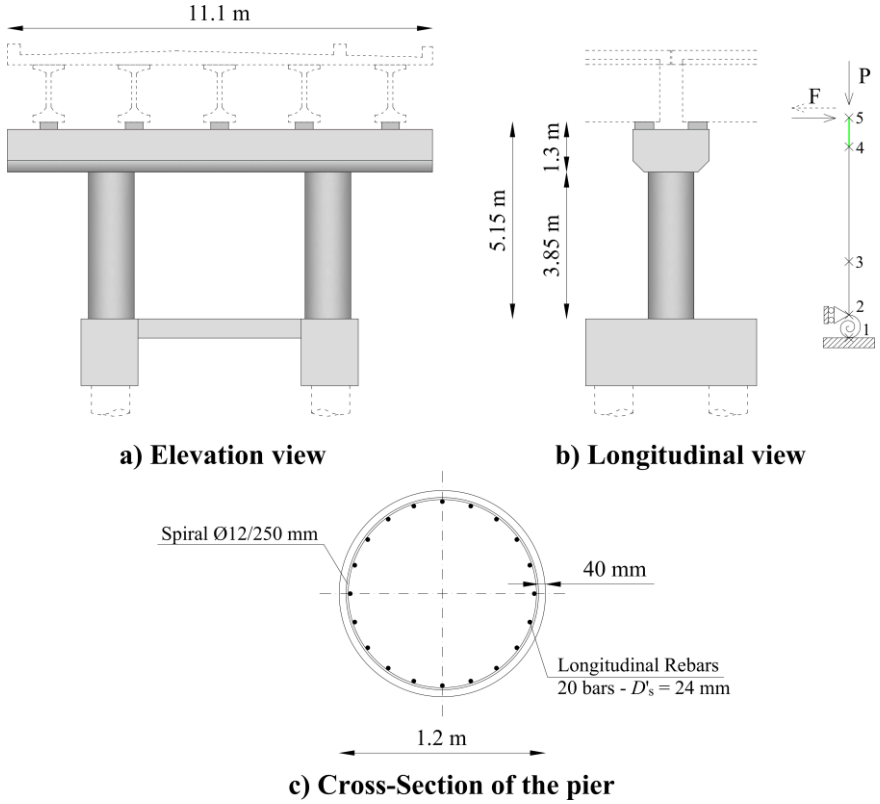

Fig. 3 Layout of the case study

4.2 Solution methods and data

The time evolution of the pitting corrosion in the RC bridge column cross-section was assessed by means of multiphysics simulation. A null initial chloride concentration is considered within the cross-section whereas the initial value of temperature and pore relative humidity are taken as 296.15 K [23 °C] and 0.65, respectively. To represent the exposure condition close to the Mediterranean coasts, a total surface content of 7 kg/m^3 of concrete is assumed.

The parametric study is detailed in Table 1. Corrosion scenarios differ in terms of pitting corrosion pattern for the longitudinal rebars in-between the transverse reinforcement. For all scenarios, it is assumed that a severe localized corrosion occurs in the longitudinal reinforcement at the level of the transverse reinforcement, in agreement with several laboratory evidence and field surveys [13],[14],[25].

Corrosion scenario cases are labelled as follows: *1pR-X-Y* where *1p* means the number of pits on the longitudinal rebars in-between the transverse reinforcement, the next number *R* is the pitting factor considered for the additional pit in-between the transverse reinforcement (R = 6 or 8), X is the ratio between pit length and uncorroded longitudinal rebar diameter in percent (X = 50, 100 or 150) and Y is the ratio between loss of reinforcing steel bar cross-section area under generalized corrosion and that due to pitting corrosion in percent (Y = 0 or 50). The case *0p* means that there is no additional pit in-between the transverse reinforcement.

The comparison among the cases 0p, 1p6-150-0, and 1p8-100-0 is meant at investigating what is the difference if none or one pit in-between the transverse reinforcement spacing is assumed, taking also into account the influence of pitting factor. On the other hand, the comparison between case 1p6-150-0 and case 1p6-150-50 serves at understanding the influence of a simultaneous generalized corrosion.

Table 1 Corrosion scenarios for the longitudinal rebars in between the transverse reinforcement

Scenario	**Additional pitting corrosion in between transverse reinforcement**		**Generalized corrosion**
	Additional pit/pitting factor/pit position	Pit length	
0p	None	-	$\rho = 0$
1p6-150-0	One pit/$R = 6/d_p = 0.5s$	$l_p = 1.5D'_s$	$\rho = 0$
1p6-150-50	One pit/$R = 6/d_p = 0.5s$	$l_p = 1.5D'_s$	$\rho = 50$
1p8-100-0	One pit/$R = 8/d_p = 0.5s$	$l_p = 1.0D'_s$	$\rho = 0$

4.3 Parametric study

The time-dependent evolution of pitting corrosion is shown in Fig. 4. As expected, pitting corrosion is more severe for transverse reinforcement than longitudinal ones. At about $t = 90$ years, the confinement is completely corroded for a pitting factor $R = 8$.

The cycle responses in terms of drift and base shear for two limit scenarios are illustrated in Fig. 5. Scenario 0p, where the pits in the longitudinal rebars are only located at the level of the transverse reinforcement, is compared with scenario 1p8-100-0 consisting of an additional identical pit in the middle of the spiral pitch (see Fig. 1). The corrosion scenarios have an influence on the response at $t = 75$ years in terms of ductility because scenario 0p prevents the bar buckling after $t = 65$ years, instead, it always arises for the scenario 1p8-100-0. On the other hand, the long-term responses (i.e., at t = 100 years) do not depend on the corrosion scenario, because they are governed by the global rebar buckling, which arises for both scenarios.

Fig. 6 shows the role of a generalized corrosion of the longitudinal reinforcing steel bars. To this end, the scenarios consisting of two identical pits at the level of the transverse reinforcement together with a less severe pit in-between without or with generalized corrosion are considered (i.e. scenarios 1p6-150-0 and 1p6-150-50). Despite the rather large magnitude of the generalized corrosion, it seems that its effects on the column capacity and ductility are moderate. This suggests that the localized corrosion is likely the most important aspect in the cyclic behavior of the considered RC bridge column.

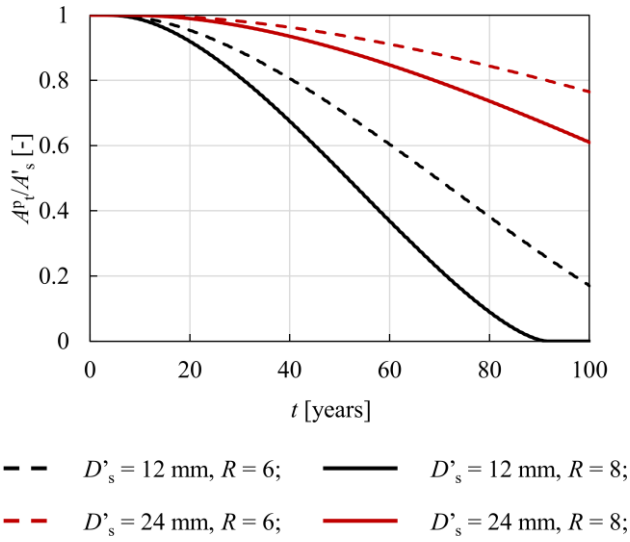

Fig. 4 Ratio of A^p_t/A'_s for longitudinal ($D'_s = 24$ mm) and transverse ($D'_s = 12$ mm) reinforcements and different values of R. A'_s is the uncorroded area of steel rebar and R is the pitting factor.

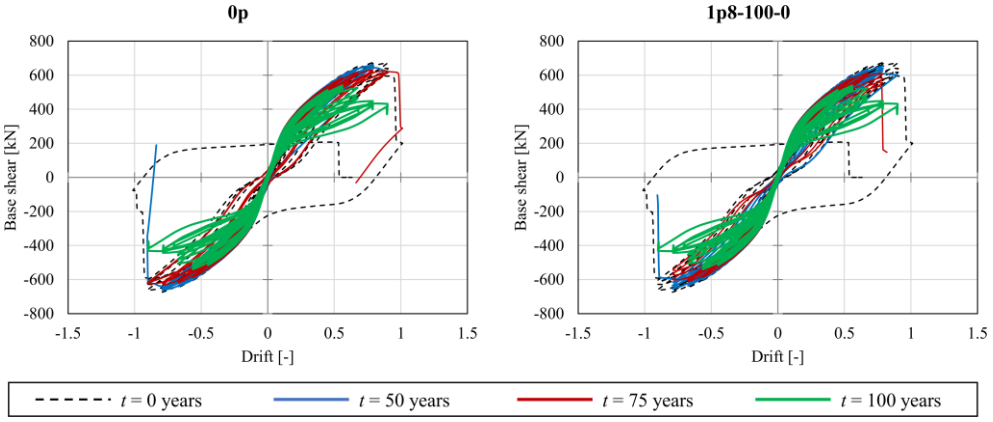

Fig. 5 Drift versus base shear for corrosion scenarios 0p (left) and 1p8-100-0 (right) at t = {0,50,75,100} years

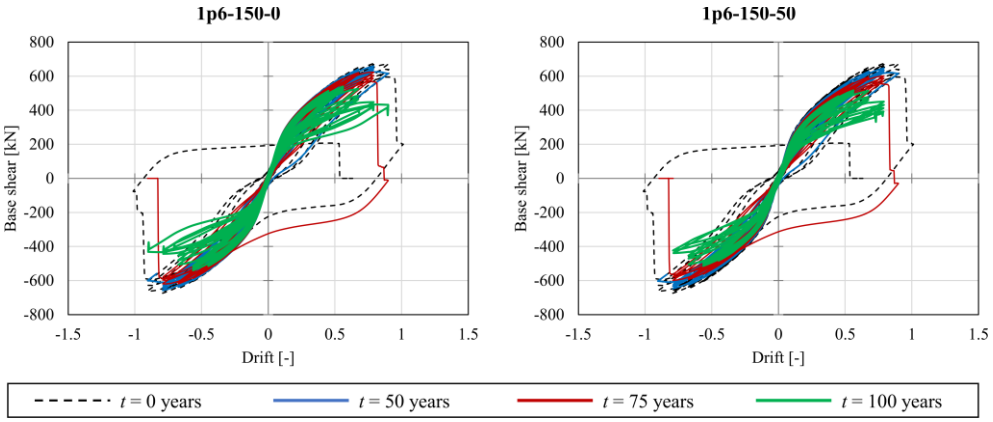

Fig. 6 Drift versus base shear for corrosion scenarios 1p6-150-0 (left) and 1p6-150-50 (right) at t = {0,50,75,100} years

5 Conclusion

In the present work, a numerical methodology for the assessment of the effects of chloride-induced corrosion on the cyclic response of RC bridge column has been presented.

A multiphysics approach has been adopted to simulate the chloride-induced corrosion. Moreover, a nonlinear model for the assessment of the RC bridge column behaviour has been developed. Finally, the proposed methodology was applied on a real case study.

Different corrosion scenarios were analysed with the purpose of unfolding the key aspects related to the response of corroded RC bridge piers. The main finding can be summarized as follows:

- Generalized corrosion has a moderate influence on the capacity and even less on ductility;
- The worst effects are due to localized corrosion which governs the flexural behaviour of the selected RC bridge column;
- The corroded ultimate tensile strain was never attained in the longitudinal rebars; hence, the behaviour of the selected RC bridge column was very sensitive to the longitudinal bar buckling;
- However, failure under tension may happen for different geometry of the RC bridge column cross-section or axial load level.

Author Contributions

Conceptualization, A.P. and G.Q.; methodology, A.P., G.Q., A.R., C.P.C. and G.F.; resources G.F.G, B.B., C.N., D.L. and A.V.B.; software analysis, A.P. and G.Q.; writing, A.P., A.R. and G.Q. All authors have contributed substantially to the work reported. All authors have read and agreed to the published version of the manuscript

References

[1] Alogdianakis F, Charmpis DC, Balafas I. 2020. "Macroscopic effect of distance from seacoast on bridge deterioration–statistical data assessment of structural condition recordings." *Structure* 27:319–29.

[2] Alipour A, Shafei B, Shinozuka M. 2011. "Performance evaluation of deteriorating highway bridges located in high seismic areas." *J Bridge Eng.* 16(5):597–611.

[3] Alipour A, Shafei B, Shinozuka M. 2013. "Capacity loss evaluation of reinforced concrete bridges located in extreme chloride-laden environments." *Struct Infrastruct Eng.* 9(1):8–27.

[4] Zhou X, Tu X, Chen A, Wang Y. 2019. "Numerical simulation approach for structural capacity of corroded reinforced concrete bridge." *Adv Concr Constr.* 7(1):11.

[5] Kashani MM, Lowes LN, Crewe AJ, Alexander NA. 2016. "Nonlinear fibre element modelling of RC bridge piers considering inelastic buckling of reinforcement." *Eng Struct.* 116:163–77.

[6] Rasulo A, Pelle A, Lavorato D, Fiorentino G, Nuti C, Briseghella B. 2020. "Finite element analysis of reinforced concrete bridge piers including a flexure-shear interaction model." *Appl Sci.* 10(7):2209.

[7] Kashani MM, Maddocks J, Dizaj EA. 2019. "Residual capacity of corroded reinforced concrete bridge components: state-of-the-art review." *J Bridge Eng.* 24(7):03119001.

[8] Belletti B, Vecchi F, Bandini C, Andrade C, Montero JS. 2020. "Numerical evaluation of the corrosion effects in prestressed concrete beams without shear reinforcement." *Struct Concr.* 21(5):1794–809.

[9] Rasulo, A., Pelle, A., Lavorato, D., Fiorentino, G., Nuti, C., Briseghella, B. 2020. "Seismic assessment of reinforced concrete frames: influence of shear-flexure interaction and rebar corrosion." In: *Gervasi, O., et al. (eds.) ICCSA LNCS* 12252:463–478.

[10] Rasulo, A., Pelle, A., Quaranta, G., Lavorato, D., Fiorentino, G., Nuti, C., & Briseghella, B. 2021. "The Impact of Corrosion on the Seismic Assess-ment of Reinforced Concrete Bridge Piers." In *International Conference on Computational Science and Its Applications* (pp. 718-725).

[11] Pelle A, Briseghella B, Bergami AV, Fiorentino G, Giaccu GF, Lavorato D, et al. 2021. "Time-dependent cyclic behavior of reinforced concrete bridge columns under chlorides-induced corrosion and rebars buckling." *Structural Concrete* 1–23.

[12] Liu T, Weyers RW. 1998. "Modeling the dynamic corrosion process in chloride contaminated concrete structures." *Cem Concr Res.* 28(3):365–79.

[13] Zhang R, Castel A, François R. 2009. "The corrosion pattern of reinforcement and its influence on serviceability of reinforced concrete members in chloride environment." *Cem Concr Res.* 39(11):1077–86.

[14] Chen E, Berrocal CG, Löfgren I, Lundgren K. 2020. "Correlation between concrete cracks and corrosion characteristics of steel reinforcement in pre-cracked plain and fibre-reinforced concrete beams." *Mater Struct.* 53(2):1–22.

[15] Val DV, Melchers RE. 1997. "Reliability of deteriorating RC slab bridges." *J Struct Eng.* 123(12):1638–44.

[16] Coleman J, Spacone E. 2001. "Localization issues in forcebased frame elements." *J Struct Eng.* 127(11):1257–65.

[17] Zhao J, Sritharan S. 2007. "Modeling of strain penetration effects in fiber-based analysis of reinforced concrete structures." *ACI Mater J.* 104(2):133.

[18] Berry MP, Eberhard MO. 2006. "Performance modeling strategies for modern reinforced concrete bridge columns." *PEER Report* 2007/07: Pacific Earthquake Engineering Research Center.

[19] Coronelli D, Gambarova P. 2004. "Structural assessment of corroded reinforced concrete beams: modeling guidelines." *J Struct Eng.* 130(8):1214–24

[20] Zhou Z, Nuti C, Lavorato D. 2014. "Modeling of the mechanical behavior of stainless reinforcing steel." Proc. of *10th fib International PhD Symposium in Civil Engineering* 515–520.

[21] Zhou Z. 2015. "Uniaxial material model for reinforcing bar including buckling in RC structures." PhD thesis, Roma Tre University, 2015.

[22] Lavorato D, Fiorentino G, Pelle A, Rasulo A, Bergami AV, Briseghella B, et al. 2020 "A corrosion model for the interpretation of cyclic behavior of reinforced concrete sections." *Struct Concr.* 21(5):1732–46.

[23] Dhakal RP, Maekawa K. 2002. "Reinforcement stability and fracture of cover concrete in reinforced concrete members." *J Struct Eng.* 128(10):1253–62.

[24] Kashani MM, Lowes LN, Crewe AJ, Alexander NA. 2016. "Computational modelling strategies for nonlinear response prediction of corroded circular RC bridge piers." *Adv Mater Sci Eng.* 2016:2738265.

[25] Francois R, Arliguie G. 1999. „Effect of microcracking and cracking on the development of corrosion in reinforced concrete members." *Mag Concr Res.* 51(2):143–50.